Polymer 51 (2010) 6334–6345

Contents lists available at ScienceDirect

Polymer

journal homepage: www.elsevier.com/locate/polymer

Rheological control in foaming polymeric materials: II. Semi-crystalline polymers

Ruogu Liao, Wei Yu*, Chixing Zhou

Advanced Rheology Institute, Department of Polymer Science and Engineering, Shanghai Jiao Tong University, Shanghai 200240, PR China

ARTICLE INFO

Article history:
Received 1 June 2010
Received in revised form
29 September 2010
Accepted 1 November 2010
Available online 4 November 2010

Keywords:
Polypropylene
Foam
Rheology

ABSTRACT

The influence of rheological properties and crystallization on foam structures, such as cell diameter, cell density and cell size distribution, of semi-crystalline polymer was investigated. The rheological properties of polypropylene (PP) were controlled by long chain branching (LCB) modification with free radical reaction and its crystallinity. The foaming behavior could be well correlated with the crystal structure and the rheological properties of polymers. The results showed that the long chain branching modification changed the crystallization speed, the diameter and the number of crystal and the rheological behavior as well. The interplay between the crystallization and the rheology of polymers with different chain structures can cause different nucleation mechanism in foaming. Both the cell size of linear PP and LCB PP decrease with crystallization time, and the cell density increases with crystallization time. The crystals in PPs acted as heterogeneous nucleation cites for bubbles, but the cell density of LCB PP is much higher than that of linear PP because of it higher spherulites density. The higher viscosity of branched PP further made its cell diameter smaller than that of linear one. Therefore, the foam structure can be well controlled by tuning the chain structure and crystal structures.

1. Introduction

Polymeric foams typically exhibit high impact strength, toughness and thermal stability, as well as low dielectric constant and thermal conductivity. These unique properties make them ideal for a largenumber of applications including automotive parts with high strength-to-weight ratio, sporting equipment with reduced weight and high energy absorption, food packaging and insulation with reduced material costs and low dielectric insulators for microelectronic applications. However, the applications of foam are determined by its structure, such as cell type, cell size, cell size distribution and cell density. The foam structures are strongly dependent on the foaming condition [1,2], molecular structure of polymer and corresponding rheological properties [3,4] and components of materials [5,6].

The materials used for foaming can be simply divided into two categories: single phase materials (amorphous polymer) and multi-component or multi-phase system (such as polymer blends, polymer with nucleation agents and crystalline polymer etc.). The control of amorphous polymeric foam structure has been studied in the previous paper [7]. The long relaxation process and strain-hardening behavior in elongational flow are found to be crucial in the control of foam structure, and the topology of polymer chains has been proved to be the decisive factor in molecular level. For semi-crystalline polymers, the crystallization affects not only the rheological properties of materials, but also the nucleation process. As known, crystal can act as heterogeneous nucleation agents to produce higher cell density [8–12]. According to the classic nucleation theory, the nucleating rate N_{het} is determined by certain energy barrier ΔG_{het}^* [5,13–15],

$$N_{het} = c_1 f_1 \exp\left(-\Delta G_{het}^*/k_B T\right) \tag{1}$$

$$\Delta G_{het}^* = \frac{16\pi\gamma^3}{3(P_D - P_C)^2}\frac{f(m,w)}{2} \tag{2}$$

where c_1 is a constant, is the surface tension, $\Delta P = P_D - P_C$ is the pressure difference across the bubble surface which is the driven forces for bubble growth, f(m,w) is the damping function due to the heterogeneous nucleation mechanism. f(m,w) is usually smaller than 1, which suggests that heterogeneous nucleation agent depresses nucleation energy barrier and makes nucleation easier. The damping function or energy reduction factor f(m,w)/2 is correlated with wetting angle ($m = \cos(\theta)$), relative curvature ($w = R/r^*$, which embodies the shape and size of heterogeneous nucleation agents). At the same time, the number and dispersion of nucleation agents will also influence nucleation rate.

Another important process affecting foam structure is bubble growth. To understand the role of rheology in foaming, a simple

* Corresponding author. Tel.: +86 21 54743275; fax: +86 21 54741297.
E-mail address: wyu@sjtu.edu.cn (W. Yu).

0032-3861/$ – see front matter © 2010 Elsevier Ltd. All rights reserved.
doi:10.1016/j.polymer.2010.11.001

bubble growth model for Newtonian fluid can be illustrative. As shown in Eq. (3), the change of bubble radius R is inversely proportional to the viscosity of matrix η[16].

$$\frac{dR}{dt} = \frac{R}{4\eta}\left(P_D - P_C - \frac{2\gamma}{R}\right) \quad (3)$$

The viscosity (actually rheological property especially in elongational flow) depends on molecular structure, content of foaming agent like supercritical CO_2 and crystallinity. The former two had been discussed in the previous paper [7] and little is known about the effect of crystallinity on bubble growth during foaming. Crystallization, even in the early stage with low crystallinity, has been found to affect the rheological properties greatly. Moreover, in the late stage of bubble growth, with the developing of crystallization, the viscosity becomes high enough to solidify the foam structure. On the other hand, a lot of experiments have shown that flow field has a great impact on the crystallization. The interplay between the flow field generated during cell growth/coalescence and crystallization behavior is one of the most complex problem in foaming semi-crystalline polymers. But such interplay could be important only when the time scales of cell growth and flow-induced crystallization match with each other. However, the effect of crystallization on the foaming is still unclear even when the flow effect on crystallization is not considered. Therefore, it is necessary to investigate the effects of time-dependent structures of crystals as well as the viscosity on foam structures to clarify the dominant factors in foaming the semi-crystalline polymers.

The application of supercritical CO_2 ($scCO_2$) in microcellular foaming processes is an area of significant research activity. As an environment-friendly physical foaming agent, CO_2 has many advantages, including adjustable solvent strength, plasticization, enhanced diffusion rates and a moderate critical temperature and pressure. In present work, the semi-crystalline polymer, polypropylene (PP), was long chain branching modified to obtain different rheological properties and crystal structures and then foamed by $scCO_2$. The variation of cell size, cell density and cell size distribution with viscosity and the size and number of crystal were recorded. The nucleation mode was judged by direct observation of etched foam sample. At last, classic nucleation theory was used to estimate the theoretical cell density and compared with experimental results. From these results, an effective method to control foam structure in semi-crystalline polymers can be deduced.

2. Experimental

2.1. Materials

Commercial isotactic polypropylene (*i*PP), T300 ($M_n = 8.0 \times 10^4$, $M_w = 3.3 \times 10^5$, isotacticity ≥96%), was from Shanghai Petrochemical Corporation, China. The melt flow rate (MFR) is 3.0 g/10 min measured at 2.16 kg and 230 °C. It was stabilized by addition of 0.2wt% Irganox 1010 (Ciba, Switzerland) antioxidant. 2,5-Dimethyl-2,5(tert-butylperoxy) hexane peroxide was obtained from Sinopharm Chemical Reagent Co., Ltd, whose half-life time is about 1 min at 180 °C. A kind of multi-functional monomer, pentaerythritol triacrylate (PETA), was obtained from Tianjin Kemao Chemical Reagent Company, China. Both the peroxide and PETA were used as received. CO_2 (>99.8% purity) was supplied by Chenggong Gas Company, Shanghai, China.

2.2. Experiment Procedure

Branched PP was obtained by modification of commercial *i*PP through reactive extrusion in a twin screw extruder with the extrusion temperature of 180 °C and speed at 150 rpm, respectively. The components of each sample were listed in Table 1. It has been shown that PP with long chain branching can be effectively formed by such method [17]. The products were cut into granules and then compressed into pieces of about 1 mm thickness on a hot stage under the pressure of 10 MPa and temperature of 190 °C.

Table 1
Formulation, abbreviation and grafting degree of each sample.

Samples	*i*PP (T300)	Irganox 1010 (wt %)	Peroxide (wt %)	PETA (wt %)
S0	100	0.2	0.1	0
S3	100	0.2	0.1	3

A piece of PP about 2 cm × 2 cm was put into an autoclave. CO_2 was compressed into the autoclave to about 14 MPa and then heated to 180 °C and hold for 4 h for complete absorption. The temperature was controlled at an accuracy of ±0.5 °C. After complete absorption of CO_2, the autoclave was cooled to 130 °C (pressure at this temperature is about 10 MPa) at speed about 1.7 °C/min and hold different times for samples to crystallize. At last, the autoclave was depressed quickly (the average rate is about 1.3 MPa/s) to foam the samples and then the products were taken out and put into ice water to freeze the foam structure. The variation of temperature with time in whole foaming process can be seen in Scheme 1.

In order to analyze the factors influencing foam structure, the crystallization process in supercritical carbon dioxide needs to be known clearly. As we know, supercritical carbon dioxide has great influence on crystallization, such as crystallinity [18], crystallization kinetics [19,20] and temperature [21]. It's hard to monitor the crystallization process and its viscosity changing by normal equipment. But we can find a condition at which the crystallization process is similar for normal pressure and high pressure CO_2, then we can use the crystallization process at normal pressure condition to simulate that at higher pressure. So firstly, it needs to find the crystalline temperature at atmosphere whose crystallization kinetics is the same as that at 10 MPa by high pressure DSC. The temperature cycle is the same as that in foaming process. Then the crystallization process was monitored by differential scanning calorimeter (DSC) and Polarized optical microscopy (POM) under normal pressure. For the rheology, the relative viscosity was recorded at this temperature. Although it is not the real viscosity at 10 MPa, it can reflect the trend of viscosity changing.

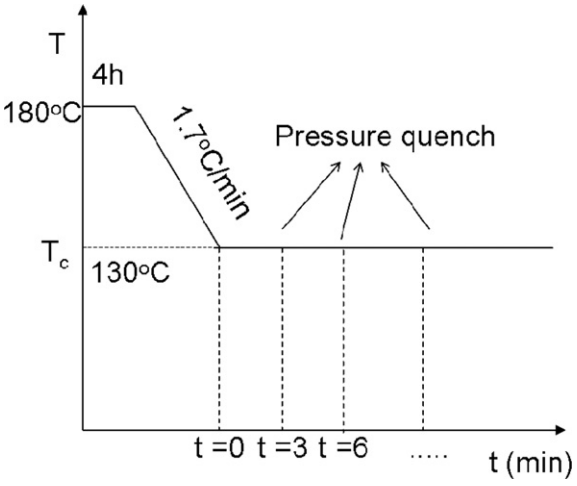

Scheme 1. Foaming process.

2.3. Differential scanning calorimetry (DSC)

Because carbon dioxide will influence the crystallization of polymer, it is necessary to know the corresponding crystallization kinetics under 10 MPa of carbon dioxide. The isothermal crystallization of S3 at 130 °C in carbon dioxide was performed on Q10P pressure DSC (TA Co., USA) under 4.8, 3.7, and 2.5 MPa, respectively. The maximum reliable pressure in the high pressure DSC used in this work is about 5 MPa, which is still much lower than that for foaming (10 MPa). The half crystallization time under different pressures in CO_2 was plotted in Fig. 1, from which the half crystallization time at 10 MPa and 130 °C can be extrapolated to be about 18.3 min. Then it was found that this is close to the half crystallization time at 146 °C under normal pressure. While for S0, the crystallization temperature was chosen at 148 °C based on the relationship of $dT_c/dP = -0.18$ K/bar [21]. The two temperatures are used in rheology measurements and polarized optical microscopy under normal pressure to simulate the foaming process under high pressure for S0 and S3, respectively.

2.4. Rheological measurements

In order to learn the rheological properties of samples used to foam, frequency sweep was carried out on a Gemini 200HR rheometer (Bohlin Instruments, UK) with parallel-plate geometry (diameter is 25 mm). Small amplitude oscillatory shear was performed in the frequency range of 0.01–100 rad/s at 180 °C. A strain of 5% was used, which was in the linear viscoelastic regime for all samples.

In order to know the variation of viscosity with crystallinity, isothermal crystallization experiments were also performed on a rheometer in oscillatory mode. The angular frequency and strain was 1 rad/s and 5%, respectively. S0 and S3 were hold at 180 °C for 5 min and then cooled to 148 °C and 146 °C at speed of 1.7 °C/min, respectively, which is the same as that of foaming process. Then the variation of viscosity with time was recorded. For convenient comparison between the two samples, the viscosity was normalized: $\eta_{rel}=\eta/\eta_0$, where η_{rel} is the relative viscosity, η the real time viscosity, and η_0 the extrapolating viscosity at the beginning of crystallization. The variation of viscosity during crystallization helps to understand the effect of rheology on bubble growth. Since the crystallization before foaming is in the supercritical CO_2 environment under high pressure, the viscosity change under the same condition should be used. However, we took use of the crystallization process under normal pressure due to the difficulty in measuring the rheological properties in melt state under high pressure. However, the crystallization process under high pressure and normal pressure should be matched, which is guaranteed by the half crystallization time as determined by DSC measurement under different pressures.

2.5. Polarized optical microscopy (POM)

Polarized optical microscope was used to observe the growth dynamics of spherulites. A thin film of one sample was heated to 180 °C at speed of 50 °C/min and hold for 5 min. Then it was cooled to 148 °C (for S0) or 146 °C (for S3) at speed of 1.7 °C/min and hold at this temperature to observe the crystallization process. At last, the diameters and numbers of spherulites can be analyzed.

2.6. Scanning electron microscopy(SEM)

SEM was used to observe the foam structure. The foamed samples were fractured after being immersed in liquid nitrogen for 30 min (to avoid the deformation or damage of the bubbles). Then the cross-sections were coated with gold and observed on a HITACHI S-2150 scanning electron microscope (Hitachi Corp., Japan). The cell size and cell density were obtained by image analysis software. For statistical accuracy, at least 50 bubbles were tested in one image. Three images were chosen for each sample and the average value was taken as the cell diameter. Because the bubbles in cross section were mostly elliptical or polygonal, the long axis was taken as the diameter of the bubbles. The cell density,N_0, in cells/cm^3 can be determined by Eq. (4):

$$N_0 = \frac{N_f}{1-V_f},\ N_f = \left(\frac{nM^2}{A}\right)^{3/2},\ V_f = \frac{\pi}{6}D^3 \times N_f \tag{4}$$

where n is the number of cells on the SEM image, M the magnification factor, A the area of the image (cm^2) and D the cell diameter.

In order to observe the nucleation mode, the fractured samples were etched in a published permanganic reagent [22–24]: a 1% (w/v) solution of potassium permanganate in an acid mixture consisting of 10 volumes of concentrated sulfuric acid, 4 volumes of orthophosphoric acid (minimum 85%), and 1 volume of water. After completely dried, the samples were coated with gold and observed on a JSM-7401F field emission scanning electron microscopy (FESEM) (JEOL Ltd., Japan).

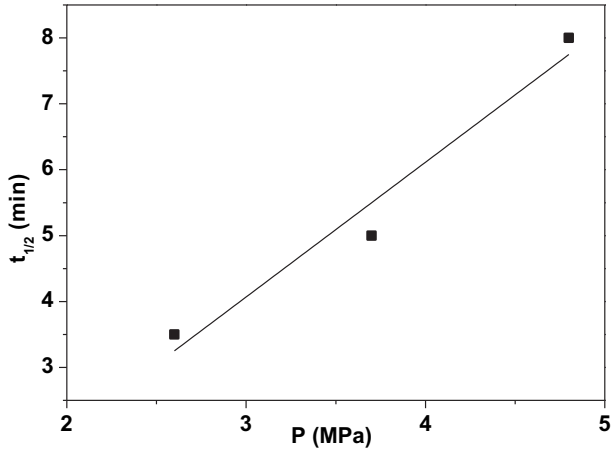

Fig. 1. The relationship between half crystallization time and carbon dioxide pressure of S3 at 130 °C.

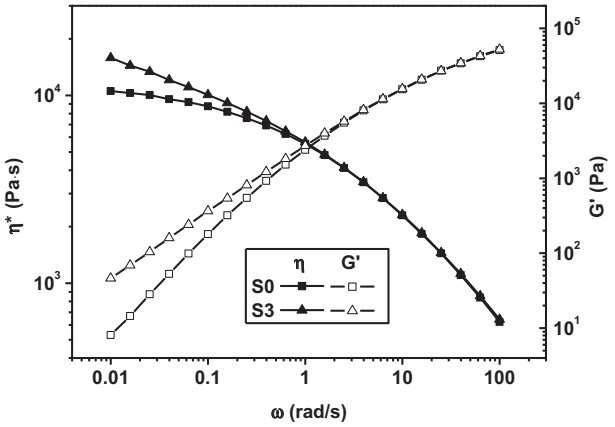

Fig. 2. Complex viscosity and storage modulus vs. angular frequency for S0 and S3 at 180 °C.

Table 2
Rheological parameters fitted by Cross model and terminal slope of storage modulus of S0 and S3, respectively.

Sample	$\eta 0/10^4$ Pa s	λ (s)	n	Terminal slope of log G'∝logω
S0	1.39	0.98	0.58	1.72
S3	2.63	26.74	0.39	0.74

3. Results and discussion

3.1. Rheological properties of melts

As discussed in introduction section, viscosity will affect bubble growth dynamics greatly, it is necessary to learn the rheological properties of foaming samples first. Fig. 2 shows the complex viscosity and storage modulus of S0 and S3 as functions of angular frequency. The higher zero shear viscosity and storage modulus of S3 at lower frequency indicate the success of modification [17]. The linear viscoelasticity of S0 shows a typical behavior of linear chain, with the terminal slope of Gr′ close to 2. The terminal slope of storage modulus of S3 at low frequency is apparently smaller than 2, showing a clear deviation from the terminal behavior of linear chains. The zero shear viscosity and characteristic relaxation time can be obtained by fitting the viscosity with the Cross model (Table 2). The enhanced zero-shear viscosity, strong shear thinning as well as the non-terminal behavior in G′ are characteristics of flexible polymers with long chain branching. It is expected that the increasing viscosity and storage modulus will hinder the bubble growth and result in small cell size according to our previous studies on amorphous polymers [7].

3.2. Influence of long chain branching on crystallization

It has been shown that introduction of long chain branching will affect not only the rheological properties of polymer, but also the kinetics of crystallization [25,26]. Fig. 3 is the POM images of sample S0 and S3 crystallized at 148 °C and 146 °C, and the isothermal crystallization time is 35 min and 15 min, respectively. The images show the different crystal structures of S0 and S3. For S0, the crystallization speed is slow at this temperature and there are only few big spherulites formed in 35 min; while at the same temperature, S3 forms much more small spherulites in 15 min. The differences of crystal structure and crystallization kinetics between S0 and S3 are obvious, which is ascribed to the branched structures of S3 [17]. Such difference in crystallization will lead to different foam structure in the end. The statistics on the growth of spherulites with time and the variation of spherulites density are shown in Fig. 4. The crystal data are also listed in Table 3. The statistical data

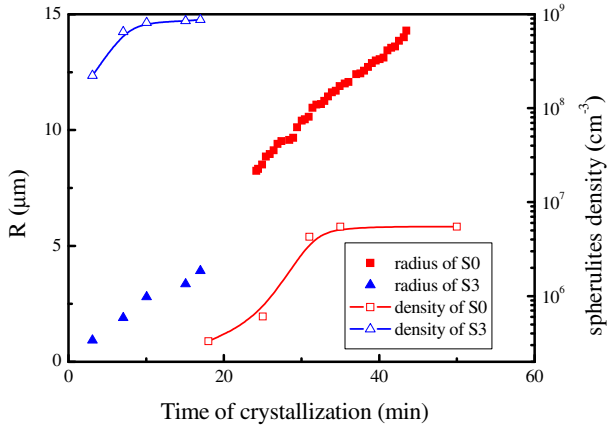

Fig. 4. The statistical data of spherulites radius and density of S0 and S3, respectively.

illustrate the whole crystallization process. It can be found that crystallization time of S3 is much shorter than that of S0 and the radius of S3 spherulites is also much smaller than that of S0. As for spherulites density, it increases with time at earlier stage and reach a plateau, and that of S3 is almost two orders of magnitude higher than that of S0. These behaviors may have great influence on the cell density of polymer foams.

3.3. Cell structure

The cell structure discussed here includes cell diameter, cell density and cell size distribution. In this section, the key points are the relationship among cell structure, viscosity, and crystal structure as well as nucleation mode.

3.3.1. Linear PP

Fig. 5 is the SEM images of foamed S0 samples with different crystallization time. From these SEM images, it can be seen that the samples with longer crystallization time before foaming have smaller cell diameter and higher cell density. The cells of shorter crystallization time samples are elongated by growth and the ratio of length and diameter is bigger. With the increase of crystallization time, the long axis of bubbles becomes shorter, and their shape change from ellipsoid to sphere. It is compared in Fig. 6 the variation of cell diameter and cell density with time with the time-dependent spherulite size, spherulite density and viscosity. It is clear that cell diameter decreases with crystallization time while the cell density increases with crystallization time. All these data are also listed in Table 3. The cell diameter decreases from 523 μm

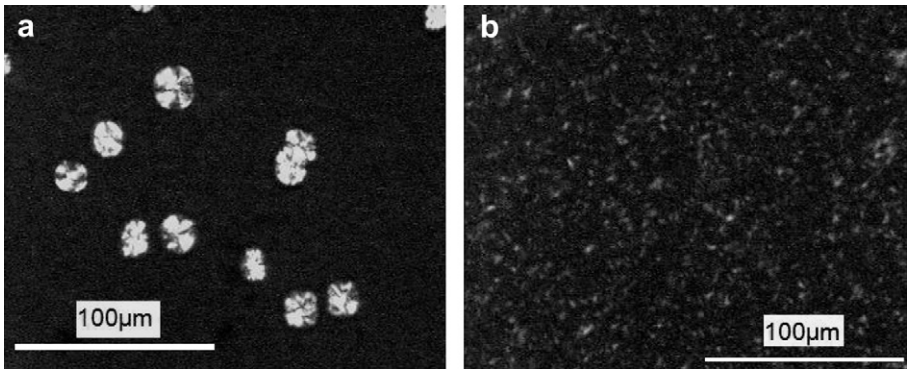

Fig. 3. POM images of S0 and S3 isothermal crystallized with different time. (a) S0, 148 °C, 35 min; (b) S3, 146 °C, 15 min.

Table 3
The structural information of S0 after crystallization for different time.

S0	t (min)[a]	18	25	31	35	50	
Spherulites diameter	D (μm)	4.80	6.97	16.50	19.15	28.28	
Spherulites density	N (10^5 cm^{-3})	0.85	1.55	10.9	14.0	14.0	
Volume fraction[b]	(%)	0.001	0.008	0.8	3.0	5.1	
	t (min)	18	25	35	90	120	240
Cell diameter	D (μm)	523.0	485.1	308.1	266.7	158.3	118.1
Cell density (exp.)	N (10^5 cm^{-3})	–	0.11	0.32	0.71	4.65	7.21
Cell density (cal.)[c]	N (10^9 cm^{-3})	0.16	0.29	2.00	25.7	25.7	
Nucleation efficiency[d]	E (10^{-4})	–	0.38	0.16	0.03	0.18	

[a] t means the isothermal crystallization time before foaming.
[b] The volume fraction is calculated from the spherulites density and diameter.
[c] The ideal cell density from heterogeneous nucleation is calculated by classic nucleation theory.
[d] Nucleation efficiency of cell is defined as the ratio between the experimental cell density and the ideal cell density.

to 118 μm when the crystallization time increases from 18 min to 240 min. The cell diameter is bigger than many other polymers, such as polystyrene studied in the previous paper [7], under this foaming condition. In fact, it is known that linear PP is difficult to prepare foams with well-defined cell structures [27–29]. This is mainly because of low viscosity and weak melt strength of polypropylene. Both the cell size and the cell density become constants for long crystallization time.

Apparently, the effect of crystallization on foaming for linear PP can be divided into two regimes. In the early stage of crystallization (stage I), the cell diameter decreases sharply, while the viscosity keep almost unchanged. This suggests that rheology is not the dominant factor in this stage. The fast decrease of cell diameter is strongly correlated with the rapid increase of the spherulite density, which increases one order of magnitude in 35 min. The formation of crystal helps to exclude the foaming agent, supercritical CO_2, into the amorphous phase near the spherulites. At the same time, the crystals can act as the heterogeneous nuclei for cell growth. In fact, both the higher concentration of $scCO_2$ near the spherulite and the heterogeneous nucleation mechanism promote a quick increase of cell density in stage I. As a result, more foaming agent is used to nucleation, and cell size becomes smaller. It is also noticed that the size of spherulite is much smaller than that of cell and the cell density is much lower than that of spherulite, which suggests that there could be a severe coalescence of cells during growth. In stage II, the cell diameter keeps decreasing with reduced speed, and the cell density gradually increases with the crystallization time. On the contrary, the spherulites density doesn't increase any more. Increase in spherulite diameter is ascribed to the continuous crystallization and results in higher crystallinity and higher viscosity. This suggests there will be no more heterogeneous nuclei in stage II than the end of stage I. It is possible that the enhancement of viscosity suppresses

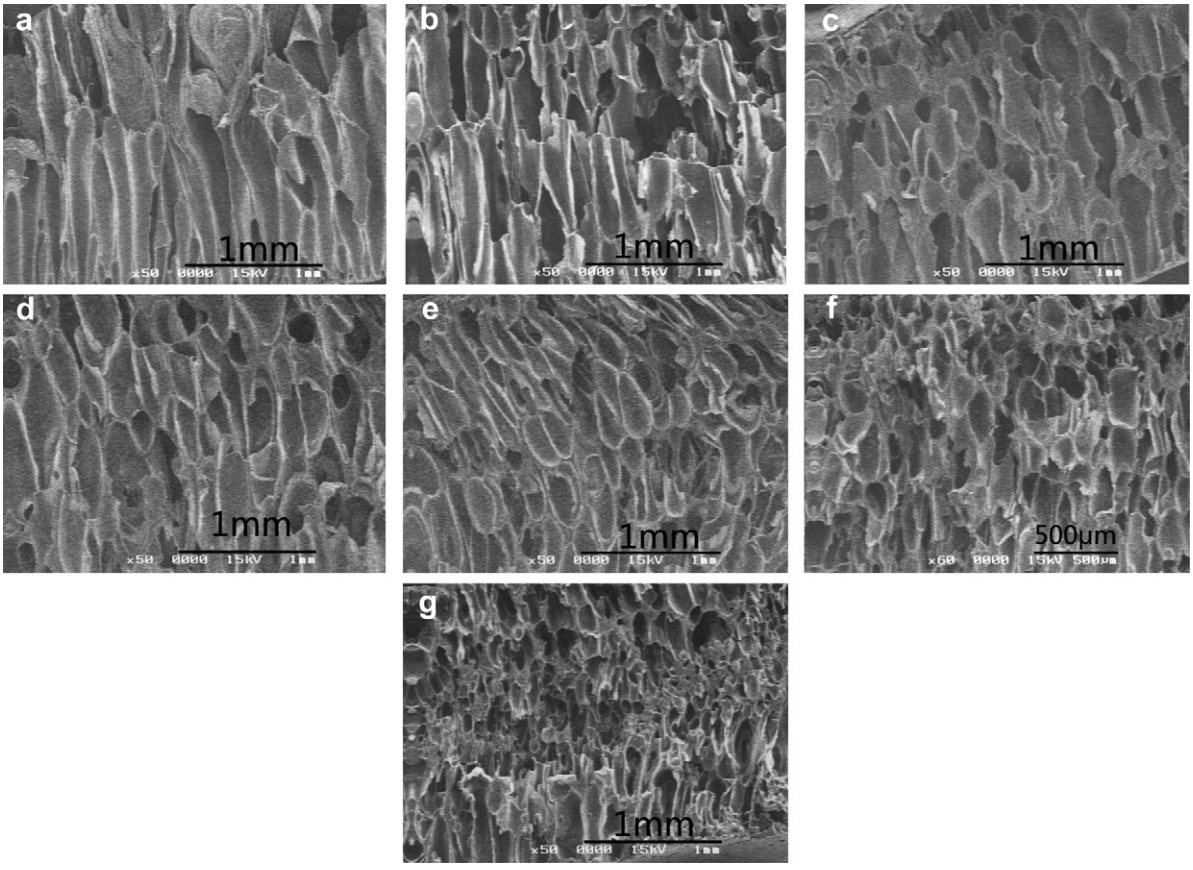

Fig. 5. SEM images of foamed S0 that crystallized for different time: (a) 3min, (b) 18min, (c) 25min, (d) 35min, (e) 90min, (f) 120min, (g) 240min.

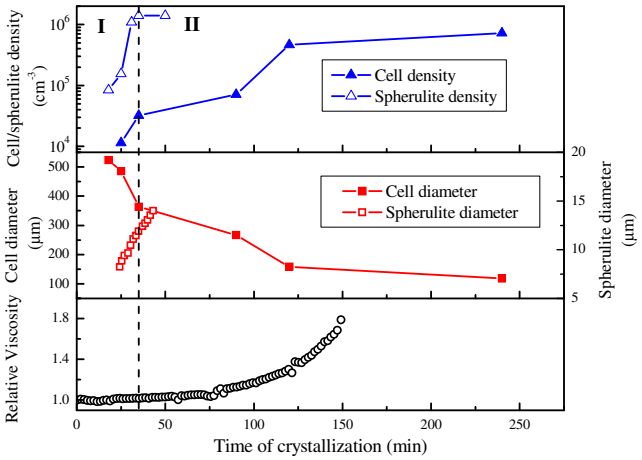

Fig. 6. The variation of cell diameter, cell density spherulite density and relative viscosity of S0 with crystallization time.

gas diffusion into bubbles and makes more gas used to nucleate. However, as known from nucleation theory and our results in previous paper [7], the influence of viscosity on cell density is very weak. A simulation result showed that cell density was still in the same order of magnitude when the viscosity increases 500 times (the simulation method is the same to that in [7] except Newtonian fluid model is used). The increase of viscosity could actually lower the possibility of cell coalescence, which results in an increase of cell density. Another possibility is the promoted cell nucleation due to the increasing concentration of foaming agent around crystalline region. Usually the higher the crystallinity, the more gas will be excluded from crystal and more cell nuclei can be formed initially. This means the possible homogeneous nucleation could increase as the crystallization proceeds. Therefore, the increase of cell density in stage II could be mainly attributed to the additional homogeneous nuclei and the less coalescence of cells during growth, which is due to the resistance during cell growth from the higher viscosity and elasticity of semi-crystalline polymer with increasing crystallinity. For long time crystallization, the cell density is still lower than that of spherulite and the cell diameter is rather large. This means that the viscosity and melt strength of linear PP have limited increases due to crystallization, which is not sufficient to obtain well-structured foams with smaller cell size and larger cell density.

In order to prove spherulites to be heterogeneous nucleation agent of bubbles, it can be achieved by the observation of etched foaming samples to find how the crystals and bubbles co-exist. Fig. 7 is the FESEM images of etched foaming samples of S0 with different crystallization time. From (a1) and (a2), which are the

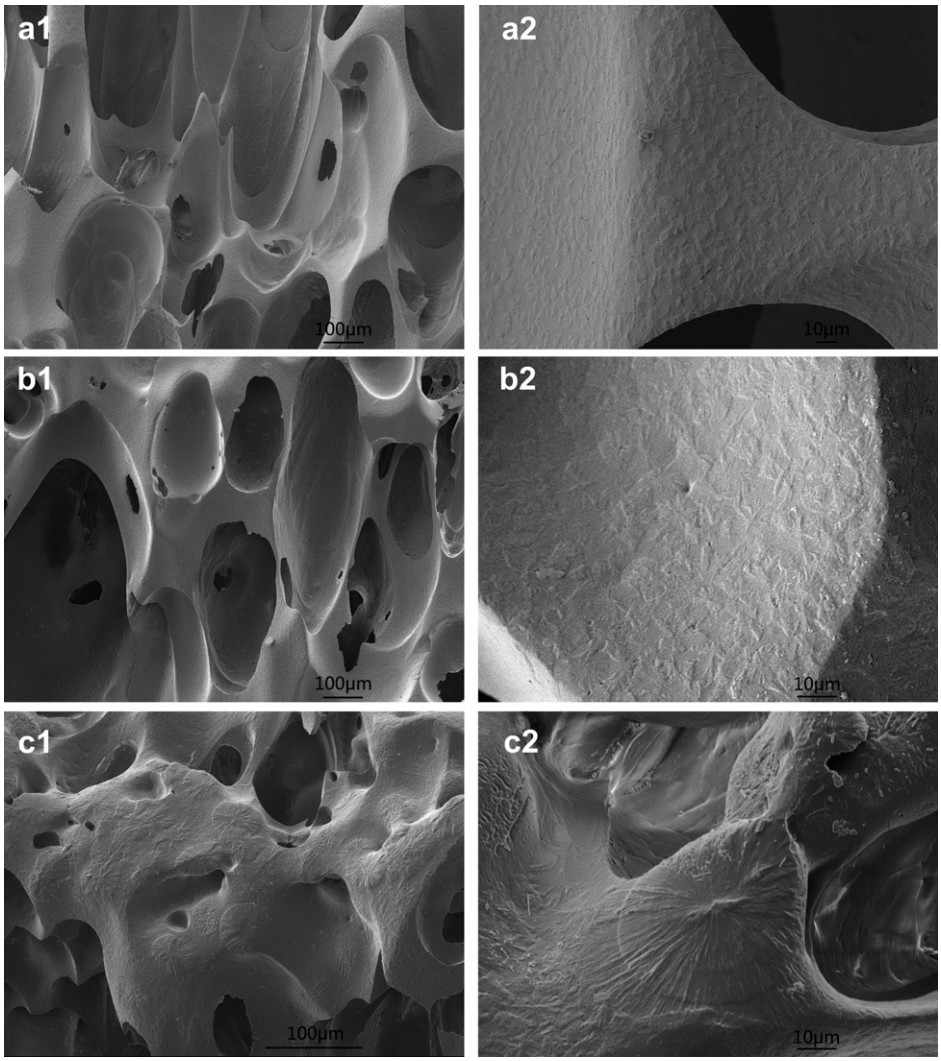

Fig. 7. FESEM images of etched foam of S0 with different crystallization time: (a1) and (a2) 35min, (b1) and (b2) 60min, (c1) and (c2) 90min.

images of the etched sample with 35 min crystallization, it is found that there are no big spherulites. This is consistent with POM images which show that the spherulites diameter is small and density is low. There is enough space for bubble to grow, which results in big bubbles. After foaming, the sample is cooled quickly, which leads to form small spherulites quickly around the bubbles (this process is the crystallization under atmosphere at 130 °C). The size of spherulites formed before and after foaming is close, so it's hard to distinguish. The images of (c1) and (c2) clearly show the morphology of etched sample with 90 min crystallization. It can be seen that there are many big spherulites among bubbles. The big crystals can be formed only after long time's crystallization, and it should be formed before foaming. By the image of higher magnification, it can be seen clearly that there co-exist big and small spherulites in the un-foamed regions. These small crystals are also formed after foaming. Each bubble is surrounded by at least one big spherulite, which is a directly proof of heterogeneous nucleation.

Cell size distribution will also affect foam properties. It is conjunctly influenced by nucleation and growth. The cell size distribution of all samples shows an almost normal distribution and it becomes narrower with increasing crystallization time. Full width at half maximum (FWHM) can be used to stand for cell size distribution and it was plotted in Fig. 8. It can be seen clearly that cell size distribution becomes narrower with increasing crystallization time. Firstly, nucleation mode changes from homogeneous to heterogeneous which makes nucleation easier and leads to higher nucleation rate. Samples with longer crystallization time have more numbers of bubbles in the same foaming time. The more gas used to nucleation, the less gas will be used to grow. Secondly, the samples with longer crystallization time have higher viscosity which will slow down the bubble growth rate and results smaller bubble diameter. Such effect of rheology on cell density has also been shown in foaming amorphous polymers [7]. Then the difference in diameter between the bubbles that nucleate and grow at different time will reduce. With the synergistic effect, the cell size distribution narrows down.

3.3.2. LCB PP

The long chain branched PP (S3) shows totally different foam structure. Fig. 9 directly shows the morphology of foam samples with different crystallization time. Cell diameter of S3 samples is obviously smaller than that of S0 and cell density is also much higher than S0. Because the crystallization rate of S3 is much quicker than that of S0, the crystallization time before foaming is much shorter than that of S0. Crystallization time of 0 min means that the pressure is released immediately when the temperature reaches 130 °C.

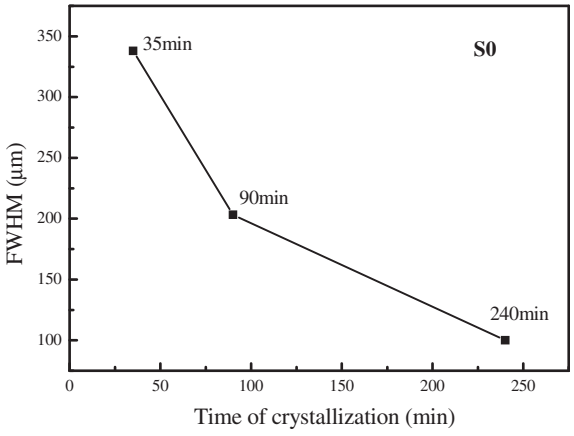

Fig. 8. Cell size distribution (FWHM) of S0 crystallized for different time.

The variation of cell diameter and cell density of S3 with crystallization time is plotted in Fig. 10. Four stages can be clearly seen according to the different crystallization time. In the early stage of crystallization (stage I), the cell diameter decreases quickly while the viscosity of polymer keeps almost unchanged. It is noticed that cell size is as low as 57 μm even without crystallization in LCB PP as compared to that of linear PP, over 500 μm after short time (3 min) of crystallization and around 120 μm after long time (4 h) crystallization. This is the.results of enhanced elasticity and retarded relaxation of long chain branching, with the effect of molecular structure has been clearly demonstrated in previous paper [7]. This phenomena suggests that long chain branching is more effective in control of the rheology, especially the elongational behavior, of polymers than crystallization for foaming process in this experimental condition, although both can significantly increase the viscosity of polymers. Both the cell density and the spherulite density increase greatly in this stage, and the size of spherulite also increase evidently. The decrease of cell diameter of LCB PP in this stage is similar to that of linear PP, i.e., increasing heterogeneous nucleation of cell on the crystal makes more foaming agent consumed in nucleation and less foaming agent can be used for cell growth. In stage II, the cell diameter keeps decreasing sharply, as compared to the slow decrease of cell diameter in linear PP (Fig. 6). The density of spherulite does not change any more in this stage, and further crystallization only cause gradual increase of spherulite size. The viscosity increases over two orders of magnitude, which is the main reason to slow down the growth of cell, lower the possibility of cell coalescence and finally reduce cell size. The huge difference in the variation of viscosity during crystallization of linear PP and LCB PP is ascribed to the difference in crystallinity (or the volume fraction of spherulite as shown in Tables 3 and 4) under the same condition. Furthermore, the difference in crystallinity between linear PP and LCB PP at the same time under the same temperature is due to the faster kinetics of crystallization of LCB PP, which is believed to be related with the branch point induced nucleation for crystallization in LCB PP [25,26]. It is also noticed that the cell size is always larger than that of spherulite both in stage I and II. However, they become comparable in size in the end of stage II due to continuous decrease of cell size and continuous increase of spherulite size. In stage III, the cell diameter decreases and the cell density increases further. Both cell diameter and cell density reach constant values for longer crystallization time. The density of spherulite does not change in this stage. Further crystallization increases the diameter of spherulite and can be illustrated by the increase of viscosity. The size of spherulite is expected to be larger than that of cell. It is noticed in this stage that the cell density is much high and even larger than the density of spherulite. There are two possibilities for such phenomena. Firstly, only heterogeneous nucleation of cell exists. More than one cell could be formed from one spherulite, which explains that the cell density is higher than the density of spherulites. This is possible since the cell size is generally smaller than the spherulite size in this stage. But from Fig. 11 (b2), it can be found that there are many crystals aggregate together and in these regions there are no bubbles. These crystals cannot be regarded as nucleation sites, which implies that the crystals are not used efficiently as heterogeneous nucleation sites. Secondly, there exists heterogeneous nucleation and homogeneous nucleation of cell simultaneously. For heterogeneous nucleation of cell, less than one cell could be formed from a spherulite on average. Additional cell in the final foams is formed via homogeneous nucleation in the amorphous regime. This is also possible since the exclusion of foaming agent into amorphous regime during crystallization makes concentration of $scCO_2$ increase and facilitates the homogeneous nucleation. As can be seen in Table 4, the volume fraction of crystal at 16.5 min is about 20% of the whole

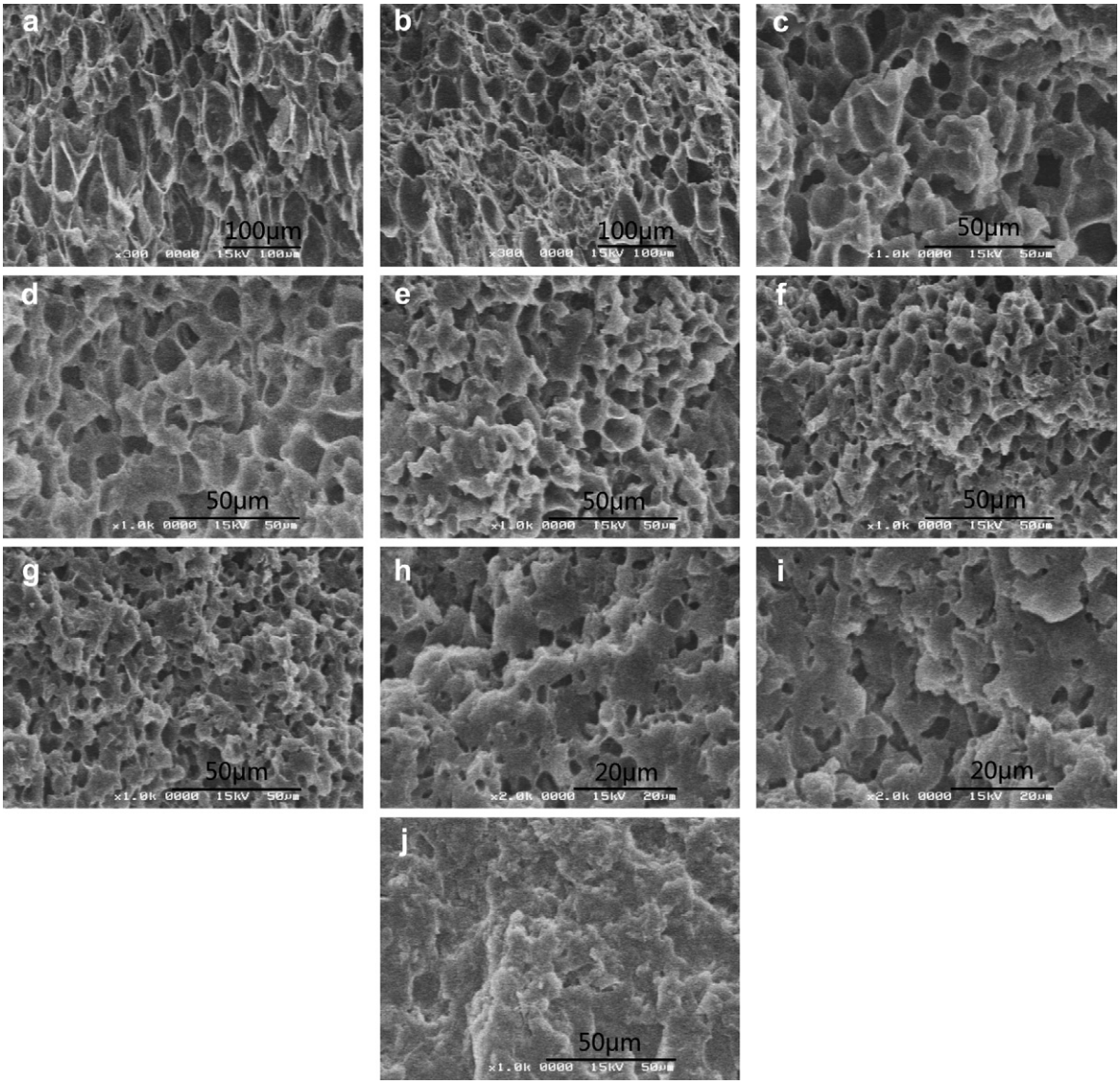

Fig. 9. SEM images of foamed S3 that crystallized for different time: (a) 0 min, (b) 3 min, (c) 6 min, (d) 10 min, (e) 15 min, (f) 16.5 min, (g) 18 min, (h) 20 min, (i) 25 min, (j) 35 min.

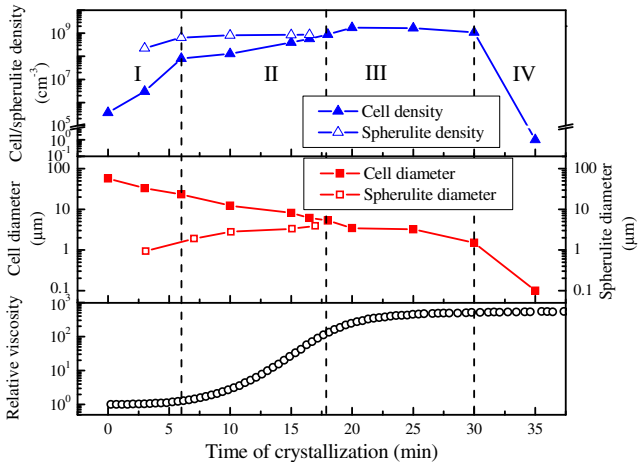

Fig. 10. The variation of cell diameter, cell density and ideal cell density of S3 with crystallization time.

matrix. The viscosity of matrix is very high at this time and makes bubble grow slowly. So more gas can be used to nucleation and form more bubble. As the crystallization time increases further, the cell size decreases with more crystallization and at last there are no bubbles in the sample with 35 min crystallization. That is the stage IV. The high degree of crystallinity leaves very limited space of amorphous regime, which prevents the growth of cell (Fig. 2).

Fig. 11 illustrated the coexistence of spherulites and bubbles of sample S3. Some information of nucleation can be found by these images. There are only small crystals in all the samples with different crystallization time. This is in accordance with POM images that the crystals of long chain branched samples are small. The first two images (a1 and a2) are those of etched sample with 3 min crystallization. The small crystals are almost the same. It's hard to judge it is formed before or after foaming. As for the sample with 15 min crystallization, the crystals are a little bigger than that with 3 min crystallization. It should be formed before foaming. After 35 min crystallization, the crystals are even bigger, and disperse uniformly in the matrix. There is almost no place for bubble to grow.

Cell size distribution for S3 plotted in Fig. 12 shows clear three regimes as discussed above. The cell size distribution becomes

Table 4
The structural information of S3 after crystallization for different time.

S3	t (min)	0	3	6	10	15	16.5	18	20	25
Spherulites diameter	D (μm)	0	1.9	3.8	5.6	6.7	7.9	–[a]	–[a]	–[a]
Spherulites density	N (10^8 cm^{-3})	0	2.23	6.49	8.15	8.49	8.73	–	–	–
Volume fraction[b]	(%)	0	0.013	1.0	5.8	9.9	20.2	–	–	–
Cell diameter	D (μm)	57.3	33.0	23.3	12.3	8.2	6.1	5.3	3.4	3.2
Cell density (exp.)	N (10^7 cm^{-3})	0.036	0.30	8.06	12.8	40.1	57.8	89.3	176	169
Cell density (cal.)[c]	N (10^{12} cm^{-3})	–	0.41	1.19	1.50	1.56	1.60	–	–	–
Nucleation efficiency[d]	E (10^{-4})	–	0.07	0.68	0.85	2.57	3.61			

[a] The data were from POM images and there were too much spherulites to account.
[b] The volume fraction is calculated from the spherulites density and diameter.
[c] The ideal cell density from heterogeneous nucleation is calculated by classic nucleation theory.
[d] Nucleation efficiency of cell is defined as the ratio between the experimental cell density and the ideal cell density.

narrower with increasing crystallization time. The increasing nucleation sites and viscosity are the reasons for this trend. It is also noticed that the cell size distributions of S3 are narrower than that of S0 samples. Higher spherulites density, viscosity and melt strength of S3 lead to this difference.

The interplay between crystallization and foaming can be schematically shown in Scheme 2, which can be summarized below.

3.3.2.1. Linear PP. Stage I: There is a low spherulite density with large spherulite size. The cell is formed mainly by the heterogeneous nucleation. The final cell density and cell size is controlled by the low viscosity and weak melt strength of linear PP, which favors the cell coalescence during foaming. The increase of cell density and decrease of cell size after different time of crystallization is mainly attributed to the increase in density of spherulite.

Stage II: The spherulite size is rather big and the density of spherulite is almost constant. Limited increase in viscosity does not change the process of cell growth and coalescence greatly. Increase of cell density and decrease of cell diameter after longer

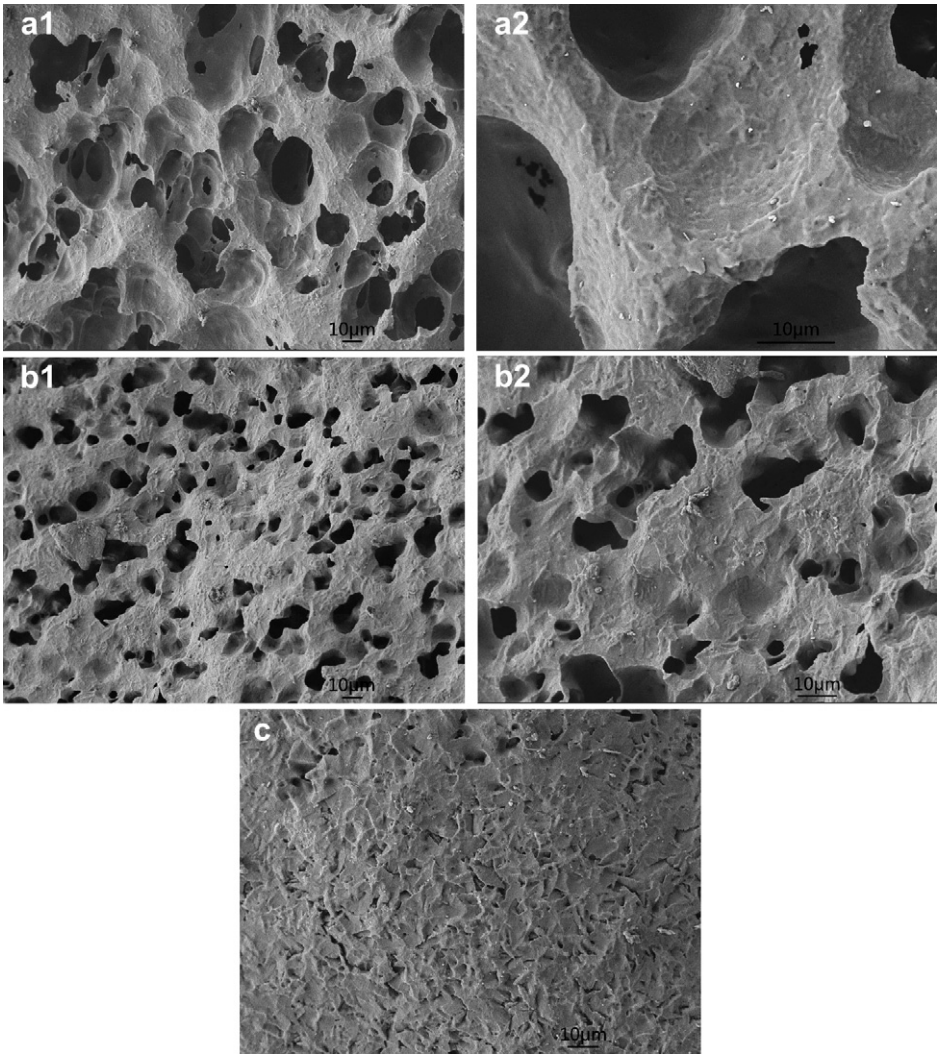

Fig. 11. FESEM images of etched foam of S3 with different crystallization time: (a1) and (a2) 3min, (b1) and (b2) 15min, (c) 35min.

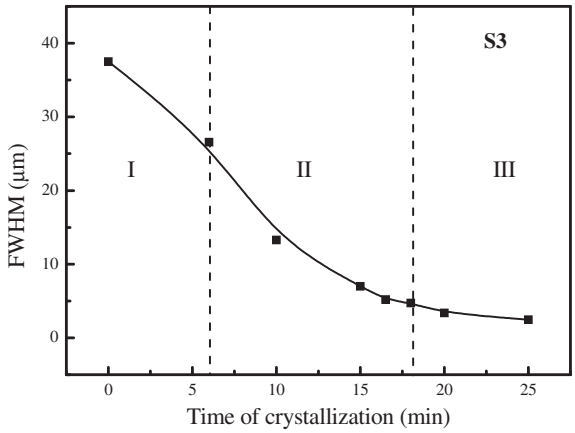

Fig. 12. Cell size distribution (FWHM) of S3 crystallized different time.

crystallization time are partly due to the limited hindrance of cell growth and coalescence by increase of viscosity, and partly ascribed to the contribution from homogeneous nucleation, since the exclusion of the foaming agent to amorphous regime cause an increase in its concentration near the spherulites as the crystallization proceeds and favors both heterogeneous nucleation and homogeneous nucleation.

3.3.2.2. LCB PP. Stage I: The density of spherulite is relatively high and the size of spherulite is quite small. Viscosity increase due to crystallization is also limited. Cell is formed mainly via heterogeneous nucleation. The final cell density and cell size are controlled by the rheology of polymer with long chain branching. The increase of cell density and decrease of cell size after longer time of crystallization is mainly attributed to the increase in density of spherulite.

Stage II: The density of spherulite is almost constant, while the size of spherulite slightly increases with annealing time. The decrease of cell size and increase of cell density is mainly attributed to the strongly enhanced viscosity due to crystallization, which

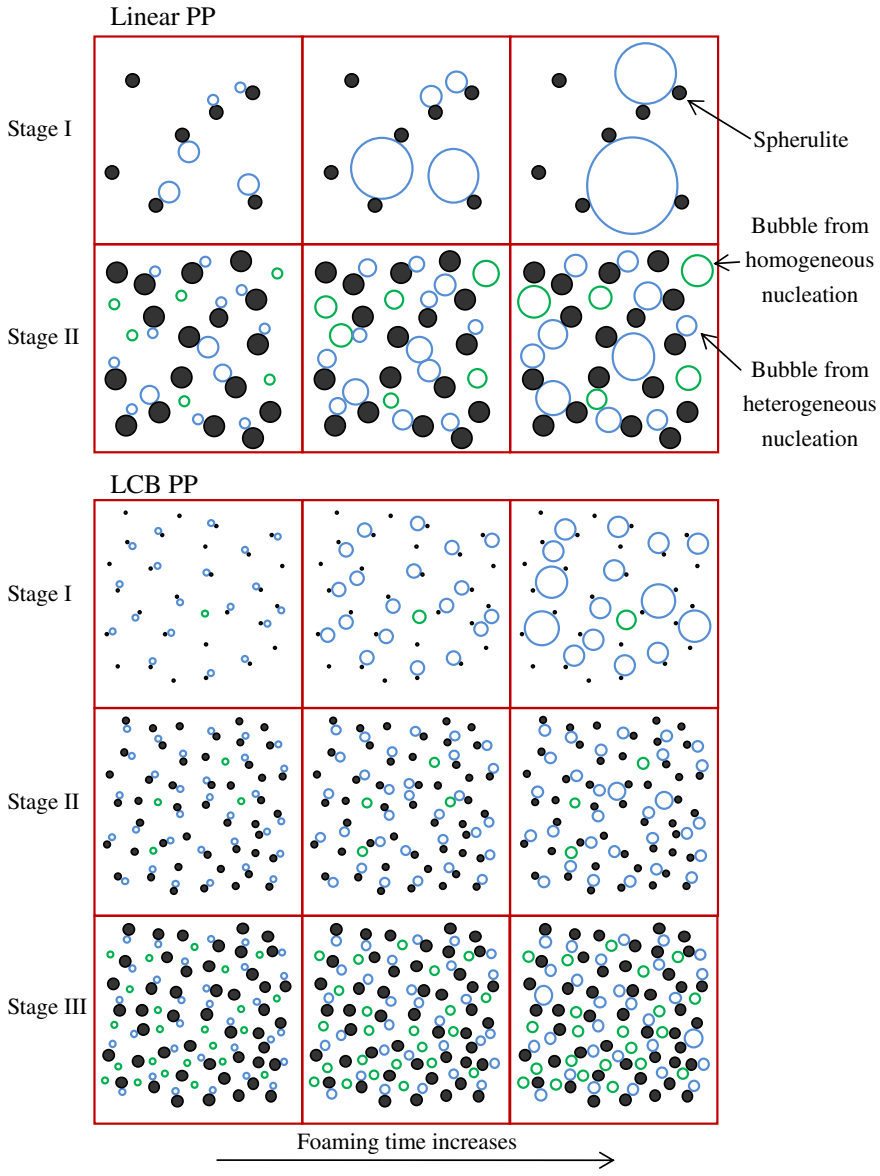

Scheme 2. Schematics of crystallization and foaming in linear PP and LCB PP.

slow down the cell growth and lower the possibility for cell coalescence.

Stage III: The density of spherulite is almost constant, while the size of spherulite slightly increases with annealing time. The cell density increases further and becomes larger than that of spherulite, which is ascribed to the large amount of homogeneous nucleation due to the exclusion of $scCO_2$ from the crystalline.

3.4. Ideal cell density from heterogeneous nucleation and nucleation efficiency

In order to compare the nucleation efficiency of crystals S0 and S3, the ideal cell density of is calculated by heterogeneous nucleation rate and nucleation time.

$$N_f = N_{het} {}^* t_c \tag{5}$$

Here, t_c is the nucleation time and N_{het} is heterogeneous nucleation rate which means the nucleus formed in unit volume and time (Eq. 1). In Eq. (1), f_1 is the frequency factor of gas molecules joining the nucleus and c_1 is the concentration of heterogeneous nucleation sites (spherulites density is taken as c_1 here). The work of forming a critical nucleus in a heterogeneous system (ΔG^*_{het}) is considered proportional to the work in a homogeneous system by a factor of f(m,w)/2 (in Eq.(2)). Here, f(m,w) is a function of the contact angle θ and the relative curvature (w) of the surface of nucleating agent (radius R) to the critical radius (r_{crit}) of the nucleated phase [5]:

$$f(m,w) = 1 + \left(\frac{1-mw}{g}\right)^3 + w^3\left[2 - 3\left(\frac{w-m}{g}\right) + \left(\frac{w-m}{g}\right)^3\right] + 3mw^2\left(\frac{w-m}{g} - 1\right) \tag{6}$$

where, $m = \cos\theta$, $w = R/r_{crit}$, $r_{crit} = 2\gamma/(P_D - P_C)$, $g = (1 + w^2 - 2mw)^{0.5}$ For crystalline polymer, the value of θ is often chosen 20° [14]. The surface tension γ is calculated to be 23.28 N/m by $\gamma = \gamma_c (1 - T/T_c)^{11/9}$ [27].

With the above equations, coupling with the data from SEM, the factor f is estimated to be about 0.0053. This is because the radius of spherulites is much bigger than the critical radius of cell (which is about 3 nm). So the decreasing of energy barrier is close to each other for the spherulites of S0 and S3. Then the difference of cell density must be caused by spherulites density.

The nucleation time t_c is about 100 times of a characteristic time τ, which can be determined by [30]

$$\tau = \frac{1}{2z^2\beta^*} \tag{7}$$

where z is the Zeldovich non-equilibrium factor and β* is the molecular jump frequency. Typical values used for z in other works are 0.01 or 0.001, and 0.01 was used here. β^* is a function of the surface tension and atomic mass of a gas molecule ((am)g), $\beta^* = 12\gamma/(am)g$. By equation (5), the ideal cell density of samples with different crystallization time can be calculated and it is listed in Tables 3 and 4. It is found that the nucleation efficiency, which is defined as the ratio of experimental cell density and calculated cell density, is in the order of 10^{-4}–10^{-5} and that of S3 is a little higher than that of S0. It is also found in Table 3 that the nucleation efficiency decreases first with the crystallization time, and then increase with it. The decrease of nucleation efficiency as the spherulite size increases is reasonable from the above heterogeneous nucleation theory. On the other hand, spherulites will collide and bubble is difficult to grow from inside when the density of spherulite increases. However, the nucleation efficiency defined here only considers heterogeneous nucleation. For a long time crystallization of S0, possible homogeneous nucleation causes the further increase of cell density, which makes the nucleation efficiency increase. The appearance of homogeneous nucleation also explains the increase of nucleation efficiency in S3 with crystallization time as shown in Table 4.

Table 5
List of symbols used in calculating cell density.

Symbol		Symbol	
ΔG^*_{het}	Hetergeneous nucleation energy barrier	k_B	Boltzmann constant
N_{het}	Nucleation rate of bubble	r_{crit}	Critical radius of nuclei
N_0	Cell density	R	Bubble radius
γ	Surface tension	w	Relative curvature
P_D	Pressure in bubble	θ	Contact angle
P_C	Atmosphere pressure	f_1	Frequency factor of gas molecules joining the nucleus
τ	Characteristic time of nucleation time	c_1	Concentration of heterogeneous nucleation sites
z	Zeldovich non-equilibrium factor	β*	Molecular jump frequency

4. Conclusions

The influence of rheological properties and crystal structure on foam structures (cell size, cell density and cell size distribution) was investigated by foaming of linear and long chain branched polypropylene with $scCO_2$ as physical foaming agent. The effect of rheology on foam structures were studied by tuning the chain structure and crystallinity. The long chain branched sample also showed different crystallization behavior as compared with linear polymer. The foam structures were strongly dependent on rheological properties as well as crystal structures. Cell diameter decreases with crystallization time while cell density increase with that for both samples. The cell density is controlled both by the spherulite density in the early stage of crystallization, and the rheology of materials that determines the coalescence of cell during foaming. The cell size is determined mainly by the rheological properties of semi-crystalline polymers, which is related to the chain structure as well as the crystal structures. The difference in the foaming process in semi-crystalline polymer is essentially controlled by the rheology of polymers in amorphous state and the crystallization behavior (Table 5).

Acknowledgement

Thanks to the support of Natural Science Foundation of China (NSFC) no. 50390095 and no. 50930002, and Shanghai Leading Academic Discipline Project (No. B202). W. Yu is supported by the SMC project of Shanghai Jiao Tong University.

References

[1] Reverchon E, Cardea S. The Journal of Supercritical Fluids 2007;40(1):144–52.
[2] Arora KA, Lesser AJ, McCarthy TJ. Macromolecules 1998;31(14):4614–20.
[3] Stafford CM, Russell TP, McCarthy TJ. Macromolecules 1999;32(22):7610–6.
[4] Di Y, Iannace S, Maio ED, Nicolais L. Macromolecular Materials and Engineering 2005;290:1083–90.
[5] Lee LJ, Zeng C, Cao X, Han X, Shen J, Xu G. Composites Science and Technology 2005;65:2344–63.
[6] Di Y, Iannace S, Maio ED, Nicolais L. Journal of Polymer Science Part B: Polymer Physics 2005;43(6):689–98.
[7] Liao R, Yu W, Zhou C. Polymer 2010;51(2):568–80.
[8] Reignier J, Tatibouet J, Gendron R. Polymer 2006;47:5012–24.
[9] Baldwin DF, Park CB, Suh NP. Polymer Engineering and Science 1996;36(11):1437–45.

[10] Baldwin DF, Park CB, Suh NP. Polymer Engineering and Science 1996;36(11):1446–53.
[11] Itoh M, Kabumoto A. Furukawa Review 2005;(28):32–8.
[12] Doroudiani S, Park CB, Kortschot M. Polymer Engineering and Science 1996;36(21):2645–62.
[13] Zhai W, Yu J, Wu L, Ma W, He J. Polymer 2006;47:7580–9.
[14] Colton JS, Suh NP. Polymer Engineering and Science 1987;27(7):500–3.
[15] Shen J, Zeng C, Lee LJ. Polymer 2005;46:5218–24.
[16] Shafi MA, Joshi K, Flumerfelt RW. Chemical Engineering Science 1997;52(4):635–44.
[17] Tian J, Yu W, Zhou C. Polymer 2006;47:7962–9.
[18] Hu X, Lesser AJ. Polymer 2004;45:2333–40.
[19] Takada M, Tanigaki M, Ohshima M. Polymer Engineering and Science 2001;41(11):1938–46.
[20] Zhang Z, Nawaby AV, Day M. Journal of Polymer Science Part B: Polymer Physics 2003;41:1518–25.
[21] Kishimotoa Y, Ishii R. Polymer 2000;41:3483–5.
[22] Weng J, Olley RH, Bassett DC, Jaaskelainen P. Journal of Polymer Science Part B: Polymer Physics 2003;41:2342–54.
[23] Huang X, Ke Q, Kim C, Zhong H, Wei P, Wang G, et al. Polymer Engineering and Science 2007;47:1052–61.
[24] Huang X, Jiang P, Kim C, Duan J, Wang G. Journal of Applied Polymer Science 2008;107:2494–9.
[25] Tian J, Yu W, Zhou C. J Macromol Sci Phys 2006;45:969–85.
[26] Tian J, Yu W, Zhou C. Journal of Applied Polymer Science 2007;104:3592–600.
[27] Zhai W, Wang H, Yu J, Dong J-Y, He J. Polymer 2008;49:3146–56.
[28] Liu C, Wei D, Zheng A, Li Y, Xiao H. Journal of Applied Polymer Science 2006;101:4114–23.
[29] Gotsis AD, Zeevenhoven BLF, Hogt AH. Polymer Engineering and Science 2004;44(5):973–82.
[30] Rodeheaver BA, Colton JS. Polymer Engineering and Science 2001;41(3):380–400.